In situ preparation and catalytic activation of copper nanoparticles from acetylide molecules

Ken Judai [a,b,*], Shigenori Numao [a], Junichi Nishijo [a], Nobuyuki Nishi [a]

[a] *Institute for Molecular Science, National Institutes of Natural Sciences and The Graduate University for Advanced Studies, Myodaiji, Nishigo-naka 38, Okazaki 444-8585, Japan*
[b] *College of Humanities and Sciences, Department of Integrated Sciences in Physics and Biology, Nihon University, Sakurajosui 3-25-40, Setagaya-ku, Tokyo 156-8550, Japan*

ARTICLE INFO

ABSTRACT

Because metal nanoparticles have a high surface area to volume ratio, they can be highly reactive, cost-effective catalysts. However, metallic surfaces are usually too reactive to maintain their metallic character in the presence of oxygen and/or water vapor. Metal nanoparticle catalysts must be handled carefully to avoid oxidation and inactivation. Here, we suggest a facile in situ preparation method for metal nanoparticle catalysts. Copper acetylide and copper methyl-acetylide molecules are based on ionic bonding, and are relatively stable in air. They can be used as a precursor of copper nanoparticles. Due to their instability at increased temperatures, subsequent annealing promotes a segregation reaction into elemental copper and carbon. Transmission electron microscopy and powder X-ray diffraction revealed that the average diameters of the Cu nanoparticles thus formed were 13.3 and 4.4 nm for C_2Cu_2 and $CuCC–CH_3$ precursors, respectively. This suggests that the substitution of acetylide molecules can control the size of the resulting copper nanoparticles. The primary advantage of this preparation method is that the functional acetylide group can reduce copper cations. No additional reducing agent is required, so no further separation process is necessary. This presents in situ preparation process. The catalytic activity of the resulting Cu nanoparticles was confirmed for a hydrogen storage system.

© 2011 Elsevier B.V. All rights reserved.

1. Introduction

Metallic nanoparticles have attracted widespread attention due to their fascinating optical, electronic, and catalytic properties [1–3]. For many applications, small nanoparticles are preferable to larger ones, because of their higher surface area to volume ratio. However, as the size of the nanoparticles decreases, the surface energy increases, favoring the aggregation of small particles or their growth into larger particles. It is difficult to keep small nanoparticles separated. In addition to their surface energy, the chemical reactivity of nanoparticles also depends upon their sizes, and smaller particles are generally much more chemically reactive than larger particles. This tendency interferes with the preparation of small metallic nanoparticles.

Over the past two decades, a substantial body of research has been directed toward the synthesis and application of small Au and Ag nanoparticles [1,4,5]. Brilliant achievements have been reported toward the successful control of nanoparticle size and shape [4,6,7],

as well as broad applications in sensors [8], catalysis [9], and substrates for surface-enhanced Raman scattering [10]. Copper is a highly conductive, cheap, and widely-used industrial material, with a valence electron structure similar to the other coinage metals, Au and Ag. Nevertheless, over the years, the fabrication of Cu nanoparticles has attracted less attention than that of Au and Ag nanoparticles, and remains open for more intensive investigation.

The reason for the reduced attention to the fabrication of Cu nanoparticles is that Cu is much more reactive than Au or Ag. For example, the standard electrode potential of Cu^{2+}/Cu is +0.34 V, and the potentials of Ag^+/Ag and Au^+/Au are +0.80 V and +1.69 V, respectively. Therefore, Cu nanoparticles are much more easily oxidized than Au or Ag nanoparticles. However, the higher reactivity of Cu nanoparticles gives them a tremendous potential for applications in catalysis [11–14]. Several methods have been developed for the preparation of Cu nanoparticles, including the reverse micelle method [15], polyol reduction [16], microwave-assisted synthesis [17], thermal reduction [18–20], a sputtering aggregation source in the gas phase [21], and capping ligand protection techniques [22,23]. Very recently, Barron et al. reported ultra-small Cu nanoparticle production, controlled by a surfactant template and carbon nanotubes [24]. Elemental analysis by powder X-ray diffraction (XRD) [25] and X-ray photoelectron spectroscopy (XPS) [24] in those studies showed oxide contamination peaks caused by partial

* Corresponding author at: College of Humanities and Sciences, Department of Integrated Sciences in Physics and Biology, Nihon University, Sakurajosui 3-25-40, Setagaya-ku, Tokyo 156-8550, Japan. Tel.: +81 3 5317 9383; fax: +81 3 5317 9432.
E-mail address: judai@chs.nihon-u.ac.jp (K. Judai).

oxidation of the Cu nanoparticles. In most of the above methods, it was quite difficult to prevent the Cu nanoparticles from oxidizing. Yang et al. made use of this oxidation tendency to produce core–shell and hollow nanostructures of copper and copper oxide [26].

In this study, we suggest a facile method of preparing metallic Cu nanoparticles for application in catalysis. Copper acetylide (C_2Cu_2) molecules and copper methyl-acetylide ($CuCC–CH_3$) molecules can be used as precursors of Cu nanoparticles. Due to their instability at higher temperatures, annealing at 200 °C causes a segregation reaction into copper and amorphous carbon. Transmission electron microscopy (TEM) and XRD measurements revealed that the average diameter of the Cu nanoparticles produced were 13.3 and 4.4 nm from C_2Cu_2 and $CuCC–CH_3$ precursors, respectively. This indicates that the substituent of the acetylide molecules can be used to control the size of the nanoparticles. An advantage of this preparation method is that the acetylide functional groups can reduce copper cations. Therefore, an additional reducing agent is not required, removing the necessity of an additional separation process, making in situ preparation possible. The preparation of reactive Cu nanoparticles promises new applications for chemical reactions such as catalysis.

2. Experimental

2.1. Preparation of precursors

Copper(I) chloride (CuCl, 1 g, >95%, Kanto Chemical Co. Inc.) was dissolved in 5% aqueous ammonia (NH_3, 100 mL, Kanto Chemical Co. Inc.) solution in a separable flask of 500 mL inner volume. First, pure Ar gas was bubbled through the solution at a flow rate of 50 mL/min for 30 min in order to reduce the residual oxygen in the solution and in the gaseous space of the flask. Then, 1% acetylene (C_2H_2) gas or 10% methyl-acetylene, propyne ($HCC–CH_3$) gas in Ar was introduced into the reactor at an extremely slow flow rate (5 mL/min). The gas flow was controlled using a digital mass flow controller (CMQ9200, Yamatake Corp.). The solution was stirred at 300 rpm continuously during gas injection. A dark-brown (C_2Cu_2) or light-yellow ($CuCC–CH_3$) precipitate was produced after 3 h. The solid product was suction-filtered and washed with distilled water and methanol. The obtained precipitate was suspended in 50 mL of methanol in an ultrasonic bath, and was filtered again. Subsequently the precipitate was dried in a vacuum desiccator (yields ~50 mg). Caution: the C_2Cu_2 product is highly explosive. On drying, the sample becomes much more dangerous. Do not handle large amounts of C_2Cu_2.

2.2. Conversion to Cu nanoparticles

The acetylide product (C_2Cu_2 or $CuCC–CH_3$) was placed in a quartz glass tube (inner diameter 30 mm), and the tube was evacuated by a turbo molecular pump (TSU 071, Pfeiffer). Under high vacuum (below 10^{-4} Pa), the acetylides were annealed at 100–200 °C for 12–24 h in an electric tube furnace (FUT552FA, ADVANTEC Toyo Corp.). The segregation reaction during annealing formed Cu nanoparticles covered with amorphous carbon polymers.

2.3. Characterization

The obtained Cu nanoparticles were examined by transmission electron microscopy (TEM), X-ray diffraction (XRD), and UV–visible absorption spectroscopy. TEM imaging and electron energy loss spectroscopy (EELS) were carried out using a TEM apparatus with a 300 kV electron beam (JEM-3200FS, JEOL). XRD was performed with a Mo Kα line irradiated upon a glass capillary containing a powder
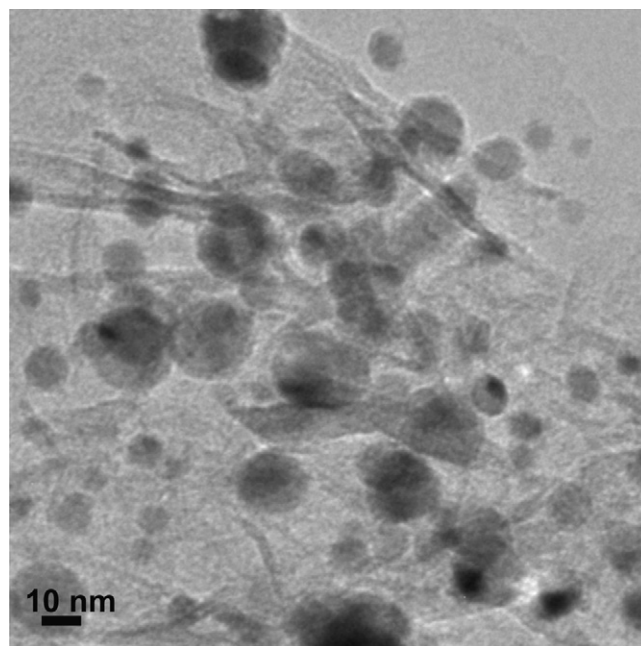

Fig. 1. TEM image of annealed C_2Cu_2. The annealing of acetylide molecules in a vacuum causes a segregation reaction to form copper and carbon. The resulting Cu nanoparticles were observed to have a spherical shape.

sample (Mercury CCD-1 R-AXIS IV, Rigaku). UV–visible absorption spectra were obtained using an integrating sphere with a sample suspended in chloroform (UV-3600, Shimazu).

2.4. Catalytic activity

The Cu nanoparticles were evaluated as a catalyst for hydrogen storage materials. Magnesium hydride (MgH_2) and 10 wt.% of the Cu nanoparticles were mixed by milling with stainless steel balls for 24 h. Hydrogen absorption and desorption rates were measured using a PCT measurement system (PCT-2SDWIN, Suzuki Shokan). A reference measurement was made for a sample of only MgH_2 without Cu nanoparticles, in order to extract the catalytic enhancement from the particle size dependence of the absorption and desorption rates.

3. Results and discussion

Fig. 1 shows a TEM image of annealed C_2Cu_2 product. Our previous study revealed that C_2Cu_2 molecules self-assemble into a nanowire morphology, and annealing at 80–100 °C promotes a segregation reaction into copper and carbon elements [27–30]. The morphology of homogenous C_2Cu_2 nanowires was converted to inhomogeneous nanocables, which were metallic Cu nanowires covered with amorphous carbon [27]. In this study, C_2Cu_2 acetylide nanowires were heated to 200 °C, at which the shape of the metallic Cu nanowires could not be maintained. Spherical Cu nanoparticles were observed as dark spots, as shown in Fig. 1. The initial structure of the nanowires remained in the TEM image as brighter regions, which can be considered as carbon fibers. Because the covalent carbon bond has a binding direction, this morphology could be maintained at the annealing temperature.

The substituent effect of acetylide molecules was examined for the nanofabrication by changing the substituent from acetylene to methyl-acetylene. Fig. 2 shows a TEM image of annealed $CuCC–CH_3$ product. Because some of the Cu nanoparticles could migrate on the surface of the TEM grid, the image shown in Fig. 2 contained no carbon fibers like those shown in Fig. 1. The diameters of the

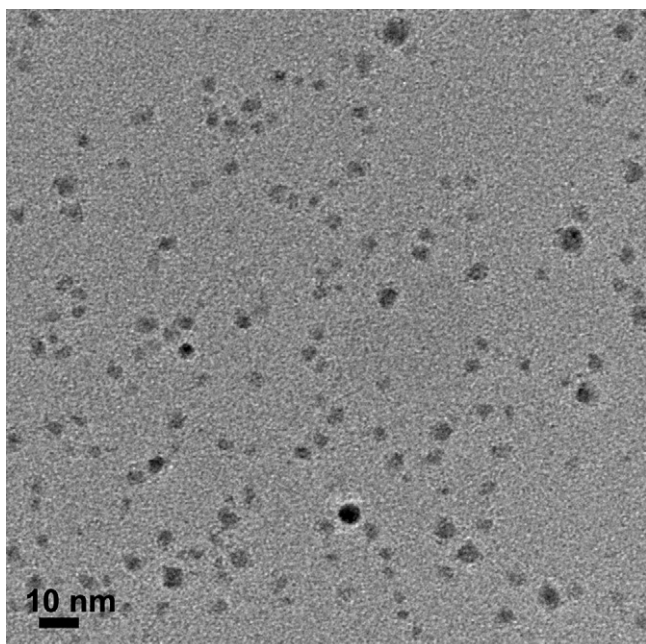**Fig. 2.** TEM image of annealed CuCC–CH$_3$. The Cu nanoparticles converted from CuCC–CH$_3$ were much smaller than those converted from C$_2$Cu$_2$.
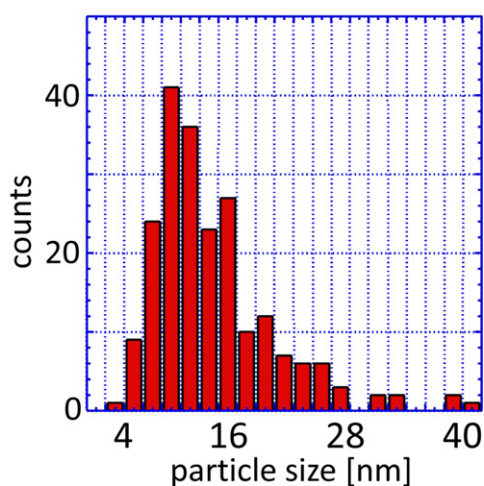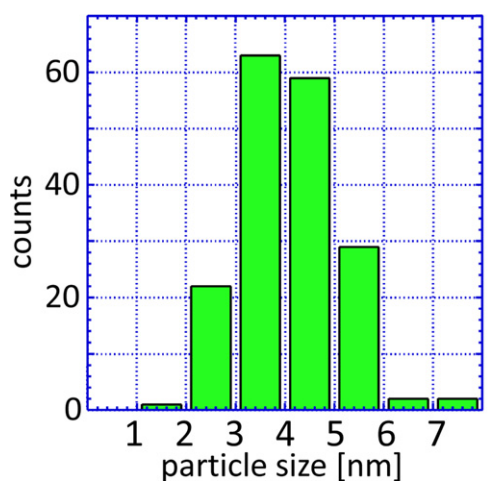

Fig. 3. Size distribution of Cu nanoparticles converted from C$_2$Cu$_2$ (bottom) and CuCC–CH$_3$ (top). The diameters of the nanoparticles were counted in the TEM images. The mean diameter of the Cu nanoparticles were 4.1 nm and 13.3 nm for CuCC–CH$_3$ and C$_2$Cu$_2$, respectively.
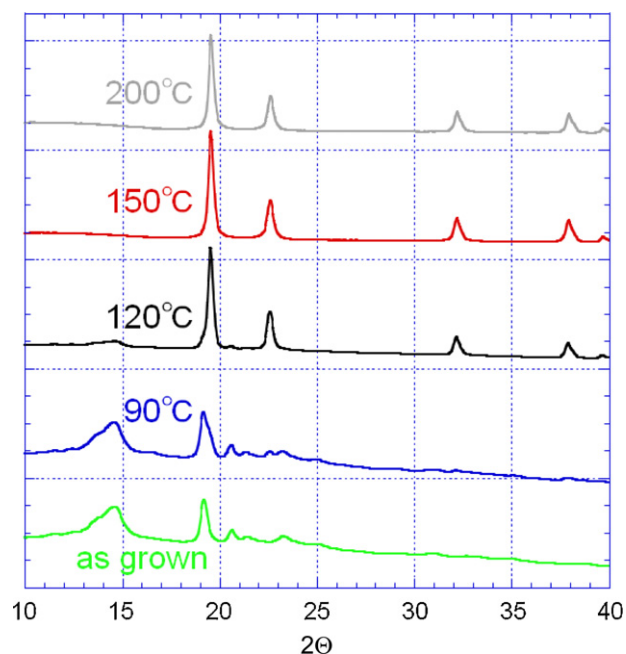

Fig. 4. X-ray diffraction patterns of C$_2$Cu$_2$ as a function of annealing temperature. Each sample was heated by an electric furnace in a vacuum for 12 h. A metallic copper fcc diffraction pattern appeared after heating above 100 °C. The segregation reaction of C$_2$Cu$_2$ should occur around that temperature.

Cu nanoparticles were measured and counted. Fig. 3 shows the size distribution of Cu nanoparticles formed from C$_2$Cu$_2$ and CuCC–CH$_3$. The numerical average diameters of the Cu nanoparticles were 4.1 nm and 13.3 nm for CuCC–CH$_3$ and C$_2$Cu$_2$, respectively. The methyl functional group substitution on the acetylide significantly decreased the size of the Cu nanoparticles formed by the segregation reaction. Furthermore, the size dispersion of the nano-particles was improved by the methyl substitution. The size distribution of C$_2$Cu$_2$, shown at the bottom of Fig. 3, included far larger particles of around 40 nm, 3 times the average size of 13.3 nm. There were no such large particles from CuCC–CH$_3$. Therefore, the substitution of acetylide can be used to control the size of the metal nanoparticles formed in the segregation reaction.

In order to examine the detailed segregation reaction of acetylide molecules during annealing, an XRD experiment was performed with a powder sample. Fig. 4 shows X-ray diffraction patterns of C$_2$Cu$_2$ as a function of annealing temperature. The samples were heated in an electric furnace under vacuum for 12 h at a constant temperature. The diameter of the C$_2$Cu$_2$ nanowires before annealing, in an as-grown sample, was determined to be about 5 nm in the previous study [27]. The peaks of the as-grown sample were broad due to the small nanowire diameter. The diffraction pattern began changing after increasing the temperature to 90 °C. At 120 °C, the diffraction pattern indicated an almost entirely metallic copper fcc crystal. Scherrer's equation can be used to calculate the average size of the nanoparticles from the peak width in X-ray diffraction [27]. The volume-weighted averaged diameter of the Cu nanoparticles after C$_2$Cu$_2$ annealing was calculated to be 13.3 nm from the peak width of the diffraction results. This value is in good agreement with the average diameter according to the TEM image, even though the volume weighted average calculated from Scherrer's equation usually differs by a factor of 0.9 from simple numerical averaging by TEM measurement. Furthermore, the peak widths were the same after annealing at temperatures between 120 °C and 200 °C. Therefore, the size of the Cu nanoparticles was constant in this temperature range. Usually, the annealing of nanoparticles causes an increase in their average size due to par-
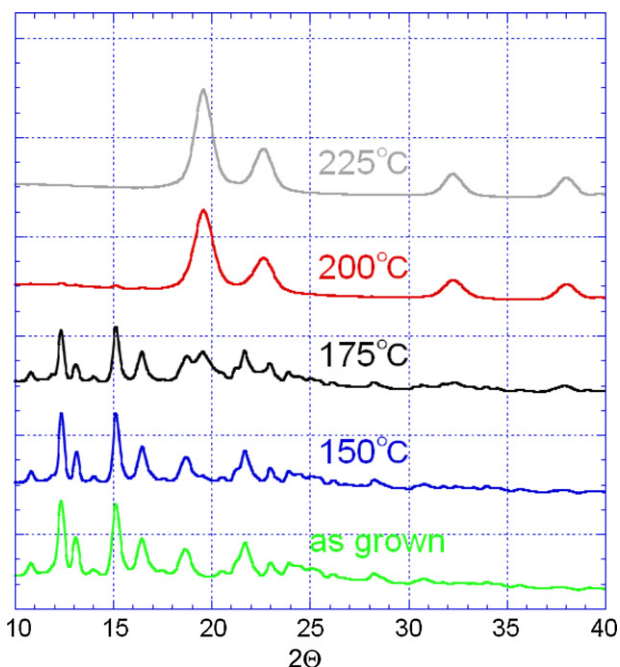
Fig. 5. X-ray diffraction patterns of annealed CuCC–CH$_3$. The segregating temperature from CuCC–CH$_3$ to metallic copper was slightly higher than that of C$_2$Cu$_2$. This reaction began around 175 °C. The peak widths of CuCC–CH$_3$ were also broader than those of C$_2$Cu$_2$. The peak widths in X-ray diffraction depend on the average size of the nanoparticles. The broader peak indicates smaller nanoparticles.

ticle growth and aggregation. Surprisingly, the Cu nanoparticles prepared by the present method did not grow during annealing.

Fig. 5 shows XRD patterns recorded from CuCC–CH$_3$ samples at various temperatures. The segregation temperature from CuCC–CH$_3$ acetylide to metallic copper was higher than that of C$_2$Cu$_2$. The reaction began around 175 °C, and the peak widths of CuCC–CH$_3$ samples were different from those of C$_2$Cu$_2$. The peak widths of as-grown CuCC–CH$_3$ samples were narrower than those of segregated copper fcc diffraction. This differed from the C$_2$Cu$_2$ diffraction peak widths. For C$_2$Cu$_2$, the peak widths of the as-grown samples were broader than those of the copper fcc nanoparticles. The size of the particles produced by the segregation reaction was unaffected by the initial size of the acetylide particles. The only effect of the substituted acetylide was to determine the size of the resulting metal nanoparticles. The average diameter of Cu nanoparticles converted from CuCC–CH$_3$ was calculated using Scherrer's equation to be 4.4 nm. This calculated average diameter, based on the peak width, was consistent with the TEM measurements. In the diffraction observations at 175 °C, the peaks for both as-grown acetylide and metallic copper co-existed. The metallic copper diffraction at 175 °C had the same peak widths as those measured at higher temperatures of 200 °C and 225 °C. The size of the Cu nanoparticles was determined at the temperature of the segregation reaction, and subsequent annealing did not result in particle growth. It is advantageous that the substitution of acetylide can control the size of the Cu nanoparticles, regardless of temperature. Therefore, nanoparticles of a given size can be used at whatever temperature their application demands. For example, nanoparticles can be created with a size appropriate for a specific catalytic reaction, and then used at the optimal temperature for that reaction.

High resolution transmission electron microscopy (HRTEM) was performed for copper nanoparticles in order to reveal their nanostructure in detail. Fig. 6 is a lattice resolved HRTEM image of a copper nanoparticle, which was observed after annealing
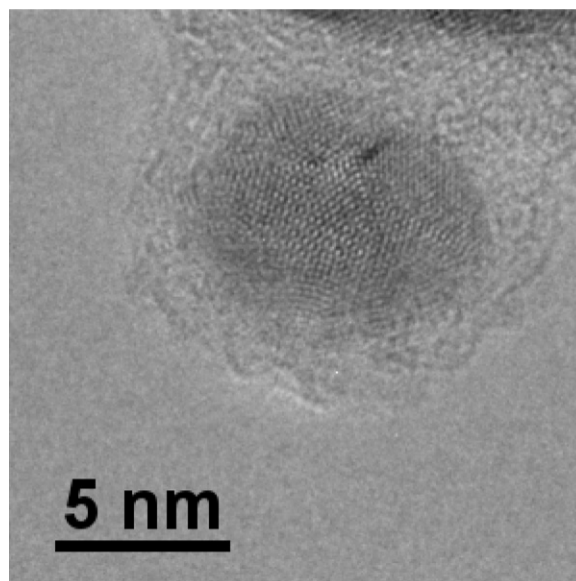

Fig. 6. Lattice resolved HRTEM image. This nanoparticle was observed after annealing CuCC–CH$_3$. In the center of the nanoparticle, an atomically-resolved lattice pattern was clearly observed. The space fringes detected in the HRTEM images matched the *d* value (0.208 nm) of Cu.

CuCC–CH$_3$. The HRTEM measurement of annealed Cu$_2$C$_2$ resulted in a similar image. In the center of the nanoparticle, an atomically-resolved lattice pattern was clearly observed. The space fringes detected in the HRTEM images were consistent with the *d* value (0.208 nm) of Cu. The diameter of the lattice-resolved metallic Cu region was 7.5 nm, slightly larger than the average particle diameter, and the Cu nanoparticle was covered with an amorphous layer. Because these nanoparticles were produced by a segregation reaction of CuCC–CH$_3$, the amorphous outer layers must consist of the organic portions of the acetylide. Acetylide contains a carbon triple bond, and the segregation reaction during annealing involves a polymerization reaction of this bond. The Cu nanoparticle was covered with the resulting amorphous carbon polymers.

Metallic copper nanoparticles are usually very reactive, and it is difficult to prevent them from oxidizing. Adding a protective layer to metallic nanoparticles, such as the amorphous carbon layers shown in the HRTEM image in Fig. 6, is one possible solution to this problem [31]. Although the TEM specimen was exposed to air during its transfer from the vacuum annealing chamber used for the segregation reaction to the TEM apparatus, the metallic copper lattice could still be observed. Furthermore, EELS measurements using the TEM apparatus detected copper and carbon signals, but not oxygen. Therefore, the amorphous carbon layers formed by the segregation of acetylide provided sufficient protection against air oxidation of the metallic copper nanoparticles.

However, strong protective layers can become an inconvenience in certain applications. For catalytic application, reactant molecules must have access to the metallic copper surface to enable catalytically activated absorption. An amorphous carbon coating may prevent contact between the copper nanoparticles and reactant molecules. The protective layer must achieve a good balance between oxidation prevention and reactant molecule access. A spectroscopic study was performed to investigate the permeability of the protective carbon layers. Fig. 7 shows UV–visible absorption spectra of Cu nanoparticles covered with amorphous carbon. The absorption spectra did change gradually because of air oxidation. The first measurement was made as soon as possible after the initial exposure to air (0 h). The initial EELS measurement after the initial exposure to air detected no oxygen, and the UV–visible absorp-
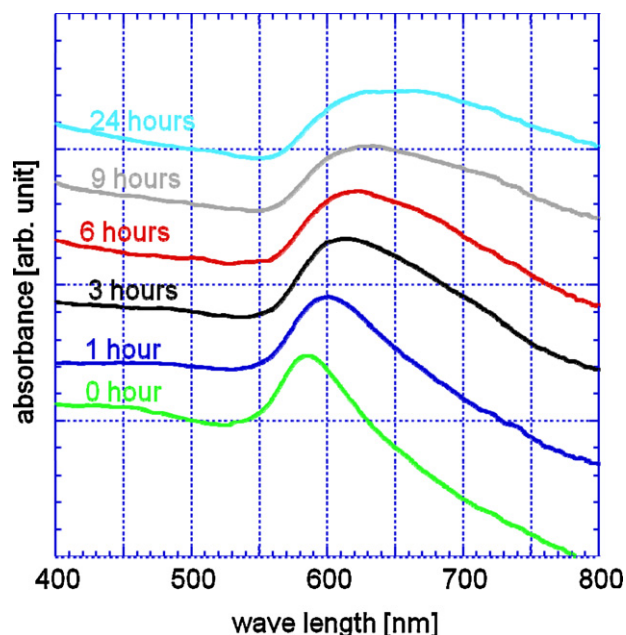
Fig. 7. UV–visible absorption spectra of Cu nanoparticles covered with amorphous carbon. The absorption spectra changed gradually because of air oxidation.

tion spectrum had a metallic copper plasmon absorption peak at 585 nm. This is a typical value for Cu nanoparticles [21,26,31]. While the Cu nanoparticles were kept in air, this plasmon peak shifted and broadened. If the surface of a metallic particle is oxidized, the metallic particle becomes surrounded by oxide layers. The permittivity of a metallic oxide layer differs from that of a protective carbon layer, because of a peak shift of the plasmon absorption by air oxidation [26]. Powder XRD measurements indicated that Cu_2O diffraction patterns overlapped with metallic copper fcc diffraction patterns after 24 h of air exposure. Elemental analysis by EELS measurements using the TEM apparatus also revealed the existence of oxygen atoms in samples with longer exposures to air. The combined results of these UV–visible absorption and EELS measurements indicate that the amorphous carbon layers can protect against the air oxidation of Cu nanoparticles, but not completely.

A hydrogen storage reaction was examined as a representative catalytic reaction [32], using Cu nanoparticles covered with amorphous carbon layers converted from acetylide molecules. There have been discrepant reports of the use of copper as a hydrogen absorption and desorption catalyst. Some reports indicated significant enhancement of the catalytic reaction [33,34], and others did not [35]. Because copper surfaces are easily oxidized, the experimental conditions may have been different. The use of Cu nanoparticles with protective carbon layers is a promising method of observing the catalytic activity without the influence of oxidation. Cu nanoparticles were mixed with a fine powder of MgH_2, and the hydrogen absorption and desorption rates were observed. Fig. 8 shows the catalytic enhancement of the hydrogen storage reactions. We then performed sets of reference experiments under identical conditions. One sample was mixture of the hydrogen storage material MgH_2 and the Cu nanoparticle catalyst. The reference was a sample of only MgH_2. The MgH_2 and Cu nanoparticles were mixed by stainless steel ball milling, and the MgH_2 sample was mixed by ball milling for the same period. Since hydrogen absorption and desorption rates depend upon the MgH_2 particle size, all reference experiments were performed with the same size of MgH_2 particles. Fig. 8 indicates that the rates of both hydrogen absorption and desorption were enhanced by the addition of Cu nanoparticles. At 280 °C, the Cu nanoparticles increased the hydrogen absorption
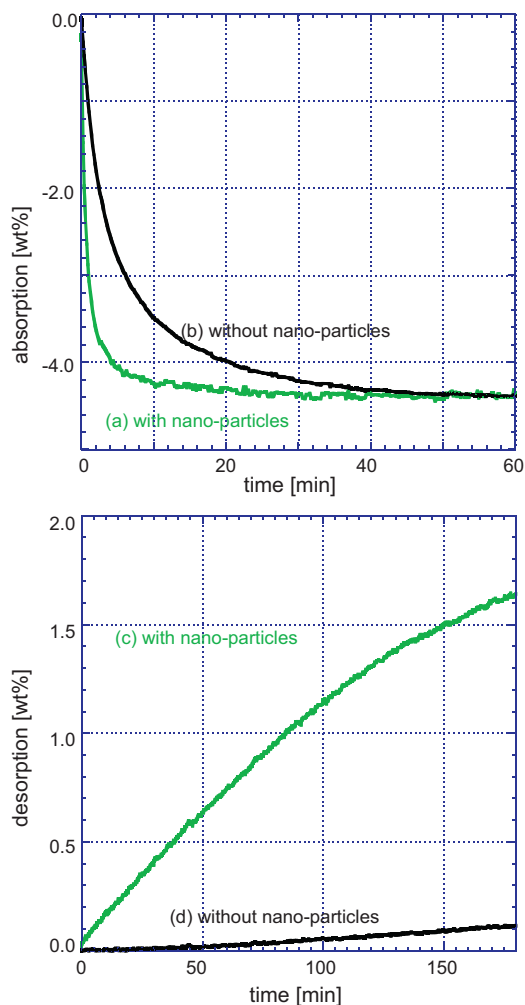

Fig. 8. Kinetics of hydrogen storage reactions. The catalytic enhancement of the chemical reactions for both hydrogen absorption (a) and desorption (c) were confirmed at the temperature of 280 °C with H_2 pressure changes in the PCT apparatus.

rate by a factor of 4, and the desorption rate was 40 times that observed for the catalyst-free reference sample. In these measurements, the Cu nanoparticles were coated with amorphous carbon layers. Therefore, the protective layer was permeable enough to allow hydrogen molecules to access the Cu nanoparticle surface and participate in the catalytic reaction. Therefore, the preparation of protected copper nanoparticles by acetylide segregation during annealing is a promising method for preparing small copper nanoparticle catalysts. The protective carbon layer can impede oxidation for several hours, which is sufficient time to allow for limited handing. However, reactant molecules for catalytic reaction can access the Cu nanoparticles through the protective layers.

4. Conclusions

In summary, we have demonstrated the in situ preparation of copper nanoparticles for catalytic applications. Copper acetylide and copper methyl-acetylide can be used as precursors of these copper nanoparticles. The average size and the size dispersion of the copper nanoparticles can be controlled by the substitution of acetylene. The product converted from methyl-acetylene had a smaller particle size (4.1 nm) and a narrower dispersion. One of the most important advantages of using an acetylide precursor is the automatic generation of amorphous carbon outer layers during the segregation reaction. These layers protect the copper nanoparticles

from oxidation, but are permeable enough that reactant molecules can access the copper nanoparticle surface to participate in catalytic reactions. Copper nanoparticles converted from acetylide were shown to function as a metallic copper catalyst.

Acknowledgments

References

[1] R. Sardar, A.M. Funston, P. Mulvaney, R.W. Murray, Langmuir 25 (2009) 13840–13851.
[2] S.A. Claridge, A.W. Castleman Jr., S.N. Khanna, C.B. Murray, A. Sen, P.S. Weiss, ACS Nano 3 (2009) 244–255.
[3] A.Z. Moshfegh, J. Phys. D: Appl. Phys. 42 (2009) 233001.
[4] M. Grzelczak, J. Pérez-Juste, P. Mulvaney, L.M. Liz-Marzán, Chem. Soc. Rev. 37 (2008) 1783–1791.
[5] W. Zhang, X. Qiao, J. Chen, Mater. Sci. Eng. B 142 (2007) 1–15.
[6] A.R. Tao, S. Habas, P. Yang, Small 4 (2008) 310–325.
[7] Y. Negishi, Y. Takasugi, S. Sato, H. Yao, K. Kimura, T. Tsukuda, J. Am. Chem. Soc. 126 (2004) 6518–6519.
[8] F.P. Zamborini, M.C. Leopold, J.F. Hicks, P.J. Kulesza, M.A. Malik, R.W. Murray, J. Am. Chem. Soc. 124 (2002) 8958–8964.
[9] M. Haruta, Chem. Rec. 3 (2003) 75–87.
[10] X.-M. Lin, Y. Cui, Y.-H. Xu, B. Ren, Z.-Q. Tian, Anal. Bioanal. Chem. 394 (2009) 1729–1745.
[11] A. Sarkar, T. Mukherjee, S. Kapoor, J. Phys. Chem. C 112 (2008) 3334–3340.
[12] B.H. Lipshutz, B.R. Taft, Angew. Chem. Int. Ed. 45 (2006) 8235–8238.
[13] J.B. Gadhe, R.B. Gupta, Int. J. Hydrogen Energy 32 (2007) 2374–2381.
[14] Y. Liu, C. Lor, Q. Fu, D. Pan, D. Lei, J. Liu, J. Lu, J. Phys. Chem. C 114 (2010) 5767–5772.
[15] I. Lisiecki, F. Billoudet, M.P. Pileni, J. Mol. Liq. 72 (1997) 251–261.
[16] M. Tsuji, S. Hikino, R. Tanabe, D. Yamaguchi, Chem. Lett. 39 (2010) 334–336.
[17] T. Nakamura, Y. Tsukahara, T. Sakata, H. Mori, Y. Kanbe, H. Bessho, Y. Wada, Bull. Chem. Soc. Jpn. 80 (2007) 224–232.
[18] S.D. Bunge, T.J. Boyle, T.J. Headley, Nano Lett. 3 (2003) 901–905.
[19] M. Salavati-Niasari, Z. Fereshteh, F. Davar, Polyhedron 28 (2009) 126–130.
[20] J. Li, C.-Y. Liu, New J. Chem. 33 (2009) 1474–1477.
[21] D.B. Pedersen, S. Wang, J. Phys. Chem. C 111 (2007) 17493–17499.
[22] O. Tzhayik, P. Sawant, S. Efrima, E. Kovalev, J.T. Klug, Langmuir 18 (2002) 3364–3369.
[23] S. Panigrahi, S. Kundu, S.K. Ghosh, S. Nath, S. Praharaj, S. Basu, T. Pal, Polyhedron 25 (2006) 1263–1269.
[24] J.J. Brege, C.E. Hamilton, C.A. Crouse, A.R. Barron, Nano Lett. 9 (2009) 2239–2242.
[25] X. Su, J. Zhao, H. Bala, Y. Zhu, Y. Gao, S. Ma, Z. Wang, J. Phys. Chem. C 111 (2007) 14689–14693.
[26] L.-I. Hung, C.-K. Tsung, W. Huang, P. Yang, Adv. Mater. 22 (2010) 1–5.
[27] K. Judai, J. Nishijo, N. Nishi, Adv. Mater. 18 (2006) 2842–2846.
[28] K. Judai, S. Numao, A. Furuya, J. Nishijo, N. Nishi, J. Am. Chem. Soc. 130 (2008) 1142–1143.
[29] J. Nishijo, O. Oishi, K. Judai, N. Nishi, Chem. Mater. 19 (2007) 4627–4629.
[30] S. Numao, K. Judai, J. Nishijo, K. Mizuuchi, N. Nishi, Carbon 47 (2009) 306–312.
[31] M. Tsuji, S. Hikino, Y. Sano, M. Horigome, Chem. Lett. 38 (2009) 518–519.
[32] A.W.C. van den Berg, C.O. Areán, Chem. Commun. (2008) 668–681.
[33] S.-J. Park, S.-J. Kim, Y.-S. Lee, M.-J. Cho, Int. J. Hydrogen Energy 33 (2008) 1706–1710.
[34] J. Hu, Q. Gao, Y. Wu, S. Song, Int. J. Hydrogen Energy 32 (2007) 1943–1948.
[35] N. Hanada, T. Ichikawa, H. Fujii, J. Phys. Chem. B 109 (2005) 7188–7194.